

Journal of 3D Printing in Medicine

The optimisation of a 3D scanning technique applied for 3D printing of bespoke medical devices

Journal:	<i>Journal of 3D Printing in Medicine</i>
Manuscript ID	3DP-2018-0026.R1
Manuscript Type:	Research Article
Keywords:	Three-dimensional surface imaging, Laser free structured-light scanner, Hand surface scan

SCHOLARONE™
Manuscripts

1
2
3
4 1 The optimisation of a 3D scanning technique applied for 3D
5
6 2 printing of bespoke medical devices
7
8
9 3
10
11

12 4 **Abstract**
13

14 5 The aim of this study is to optimise the 3D scanning process using the laser-free structured
15
16 6 light surface scanner (Artec EVA). The hand was chosen to optimise scanning protocols and
17
18 7 generate reliable high quality surface scan models. Scanning comfort, ease of scanning and
19
20 8 maximum scanning error were assessed in each hand position. Such an optimised scanning
21
22 9 method shows the potential to obtain high quality 3D hand scans quickly and reliable so that
23
24 10 they can further be used for the development of a bespoke 3D printed medical device for
25
26 11 patients.
27
28
29
30
31

32 13 **Keywords**
33

34 14 Three-dimensional surface imaging, Laser free structured-light scanner, Hand surface scan,
35
36 15 Three-dimensional printing, bespoke medical device.
37
38
39
40
41
42
43
44
45
46
47
48
49
50
51
52
53
54
55
56
57
58
59
60

1
2
3 **30 Abbreviations**
4

5 31 3D Three-dimensional
6
7 32 ANOVA Analysis of variance
8
9 33 AU Arbitrary unit
10
11 34 CAD Computer-aided design
12
13 35 CI Confidence interval
14
15 36 CT Computed tomography
16
17 37 DIPJ Distal interphalangeal joint
18
19 38 MCPJ Metacarpophalangeal joint
20
21 39 MRI Magnetic resonance imaging
22
23 40 P Position
24
25 41 PIPJ Proximal interphalangeal joint
26
27 42 SD Standard deviation
28
29
30
31
32
33
34
35
36
37
38
39
40
41
42
43
44
45

1. Introduction

The use of 3D imaging in combination with 3D printing technologies has gained popularity in various medical fields. However, obtaining reliable 3D scans to design bespoke medical devices remains challenging. “Three-dimensional surface imaging” is a process that creates and measures point cloud coordinates of object surfaces in a three-dimensional space (x, y and z). The term “three-dimensional surface imaging” needs to be clearly distinguished from the term “three-dimensional imaging” which typically refers to techniques such as magnetic resonance imaging (MRI) and computed tomography (CT) providing detailed 3D information of the internal body [1, 2].

In the 90s, the first three-dimensional surface imaging devices became commercially available [3, 4]. Ever since, researchers were dedicated to improving robustness and accuracy with the main purpose of texture visualisation and geometrical measurements. The three most commonly used surface scanning technologies for 3D body scanning are photogrammetry, Laser scanning and Millimetre wave scanner [1]. Photogrammetry projects structured light patterns onto a non-planar surface and captures the distorted pattern afterwards with a camera. This gives information of 3D surface shapes enabling an estimation of a 3D body. Laser scanning technology uses invisible, harmless laser light to measure the direction of reflection. This provides information of the distance between sensors and object surface and allows to calculate point coordinates in three-dimensional space. 3. Millimetre wave scanners uses linear-array radio-wave technology to scan a 3D object [1, 2, 5].

1.1 Medical Applications of 3D surface scanning

Initially, 3D surface scanners were developed for industrial applications such as engineering, product design and quality control. Its non-invasiveness, ease of use and commercial availability at low cost made 3D surface scanning devices popular gadgets in various medical fields such as dermatology, plastic, reconstructive and aesthetic surgery [1, 6].

Nowadays, 3D surface scanning offers various healthcare application possibilities[1] such as screening of large populations for anthropometric surveys[7], a tool for various diagnostic purposes, such as wrinkles analysis, melanoma lesion and growth defect detection[8] and wound management for the calculation of the body surface area which is an essential feature in the management of burn injuries [9, 10]. 3D Scanners can additionally be used to detect the progression and regression of chronic wounds over time [6], In the field of aesthetic surgery, 3D surface scanners are used to simulate and illustrate treatment outcomes. This can be a helpful tool to educate patients and reduce exaggerated patient expectations. The assessment

1
2
3 79 of breast volume and asymmetries with 3D surface scans can help to predict the outcome based
4
5 80 upon implant size and shape [2]. The development of bespoke medical prostheses, orthotics
6
7 81 and exoskeletons is another huge market for 3D scanning applications [11-13]. Monitoring
8
9 82 body changes over time makes 3D scanning a promising tool for dieticians, nutritionists and
10
11 83 personal coaches. It is a simple method to assess body asymmetries and muscle imbalance,
12
13 84 analyse posture and perform cross-section measurements of hip, waist and chest [1].

14 85 **1.2. 3D hand surface imaging**

15
16 86 3D surface imaging in combination with computer-aided design (CAD) and 3D printing
17
18 87 technologies are emerging for various medical applications [1]. The ability to develop bespoke
19
20 88 medical devices such as hand prosthetics, orthotics or exoskeletons is of great interest to the
21
22 89 field of modern personalised medicine [1, 11, 12]. 3D scans can potentially improve the
23
24 90 manufacturing and development process of 3D printed patient specific hand devices [12]. Low
25
26 91 cost bespoke hand prosthetic, orthotic and exoskeleton devices have the advantage of being
27
28 92 affordable for the general public. This can ultimately improve patients' compliance and
29
30 93 rehabilitation progress [14, 15].

31
32 94 However, traditionally these devices are made by using casting and moulding methods. This
33
34 95 requires a patients' appointment at the prosthetic/orthotic centres with significant time delay
35
36 96 before the device can be used by the patient. This has social and economic implications for
37
38 97 both, patients and healthcare providers. Providing a fast and easy method to accurately acquire
39
40 98 patients' hand dimensions has the potential to reduce waiting time and to allow fast delivery
41
42 99 of the devices to patients. 3D surface scanning has shown promising results in this area as
43
44 100 explained.

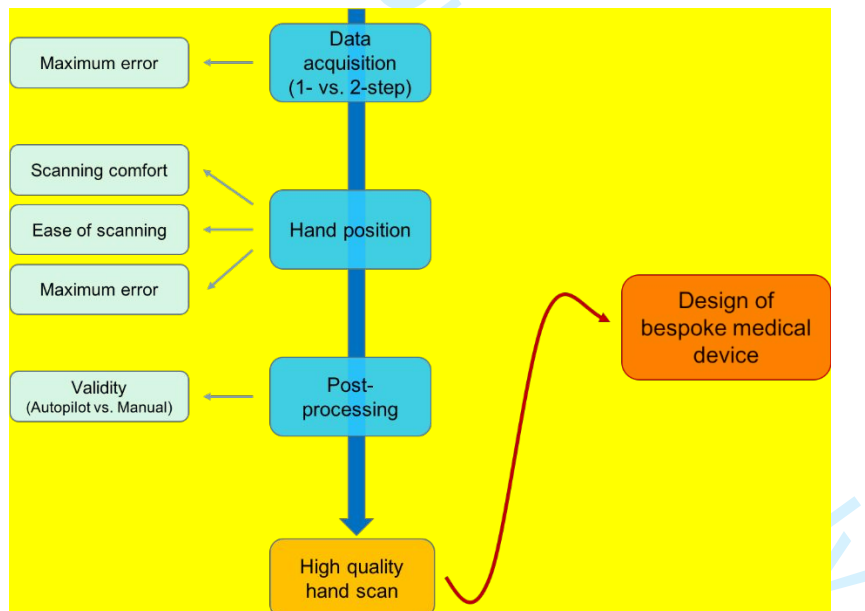
45
46 101 The scan quality has direct impact on design and manufacturing of patient specific devices,
47
48 102 especially for hands which are considered challenging objects due to their complex shape.
49
50 103 However, standardised 3D hand scanning protocols have not been established prior to this
51
52 104 study.

53
54 105 This study aims to develop easy and reliable 3D scanning protocols for using the laser free
55
56 106 structure light source based hand held scanner. Hand positioning including patient comfort and
57
58 107 accuracy of scan measurements is validated as a case study, so that the generated 3D surface
59
60 108 scan information can then be implemented into the device design and 3D printing process.

109 2. Materials and Methods

110 2.1 3D scanning

111 In this study the Artec EVA, a handheld scanner, and the software Artec Studio 12 Professional
 112 were used to obtain and process 3D surface scans of the human hand [16, 17]. The Artec EVA
 113 scanner (Artec 3D, Luxembourg) uses laser free structured-light, to obtain 3D objects [18]. It
 114 has a resolution of up to 0.5 mm, which is defined as the ability to resolve details in the scanned
 115 object and a 3D point accuracy of 0.1 mm to match the actual value of the measured quantity
 116 [16]. It has previously shown promising applications in the area of orthognatic and breast
 117 surgery [19, 20]. Single user trained in using the scanner, scanning techniques and the software
 118 features performed all scans in this study. Hand scanning was always performed on the right
 119 hand of healthy volunteers. This was done to minimise operational variabilities during scanning
 120 and data processing.



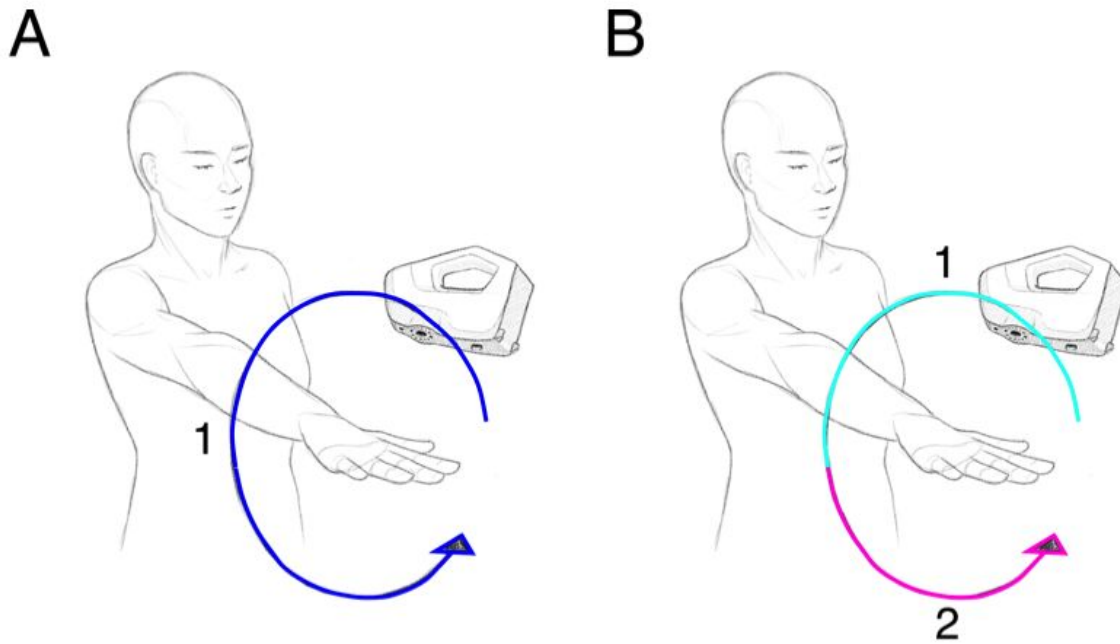
121
122 **Figure 1.** Flow chart of the proposed method.

123 2.2 Data acquisition method (1-step versus 2-step scanning)

124 Two data acquisition methods were developed, assessed and compared with each other. First,
 125 the one-step method consisting of one continuous scan orbiting the handheld scanner 360°
 126 around the hand (Figure 2A). Second, the two-step method where the scanning process is
 127 divided into two scans each of them capturing one half of the human hand surface is shown in
 128 Figure 2B.

129 Each data acquisition method was performed three times. Maximum errors resulting from those
 130 scans were used to calculate the average maximum error of each data acquisition method. All
 131 scans were performed on a single volunteer standing in an upright position with a combined

1
2
3 132 arm elevation to 90°. Scans were assessed in their original state without post-processing or any
4
5 133 other modification.
6



27 134
28 135 **Figure 2.** Data acquisition methods. A. One-step method: one continuous scan orbiting the handheld scanner 360° around the hand; B. Two-step method: the scanning process
29 136 is divided into two 180° orbits. One scan captures the dorsal aspect of the hand (1) and the other scan the palmar aspect of the hand (2). The volunteer was advised to stand
30 137 upright, perform a combined arm elevation to 90° and hold this position during the entire scanning process with the least possible hand movement.

31 138 **2.3 Hand scanning positions**

32
33 139 Six hand positions were considered feasible for 3D hand surface scanning and included in the
34
35 140 assessment. (S 1 and Figure 3)
36

37 141

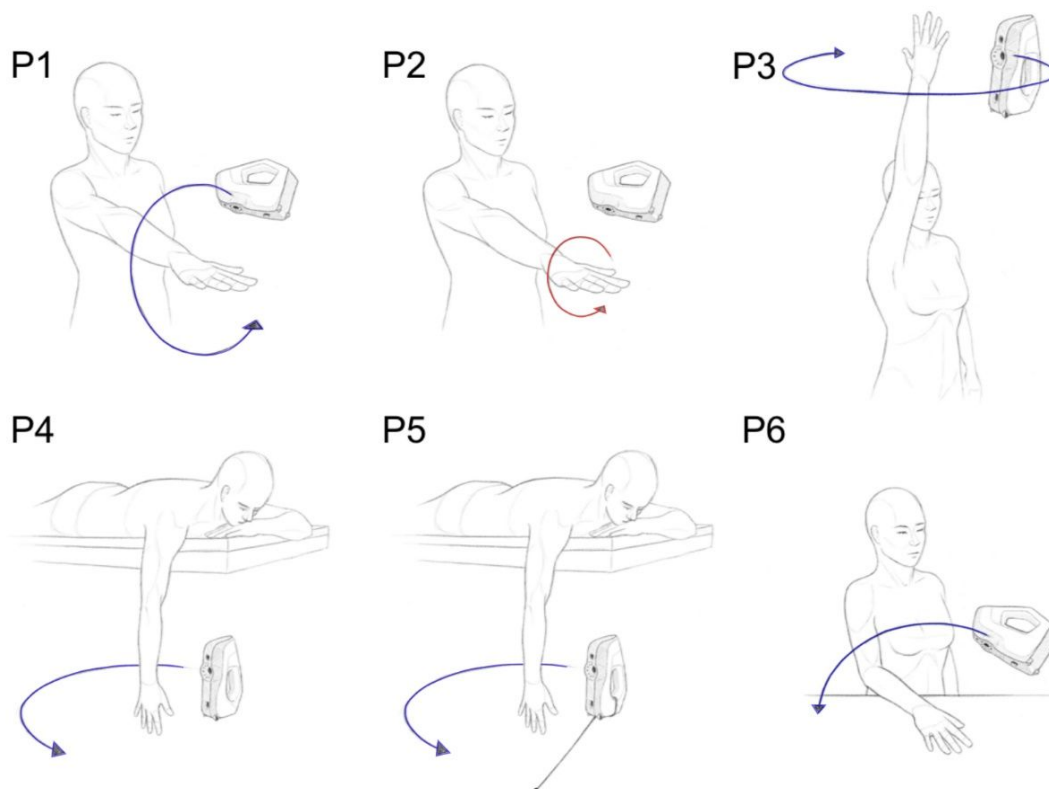


Figure 3. Figurative representation of the Hand scanning positions. **P1.** 90° arm elevation; **P2.** 90° arm elevation with full hand rotation; **P3.** 180° arm elevation; **P4.** Minimal force; **P5.** Minimal force plus guide; **P6.** Hand on surface. **Blue** indicates moving scanner; **red** indicates hand rotation.

All six hand positions were assessed and evaluated in terms of scanning comfort, ease of scanning, scan quality and duration of the scan.

2.3.1 Scanning comfort and ease of scanning

The right hand of five volunteers was scanned in all of the abovementioned positions by two users. Those five volunteers then rated the scanning process in terms of hand position comfort during the scan. Both users additionally rated the ease of the scanning process. A scaling system of 1 (worst) to 5 (best) was used to assess “scanning comfort” and “ease of scanning” for each hand position.

2.3.2 Maximum error

Three scans were performed in each hand position. This resulted in a total of 18 scans (1 user x 6 positions x 3 repetitions). The average maximum error for each hand position was calculated of those three scans. The maximum error is an Artec internal parameter in arbitrary units and can be seen as an indicator of scan quality. A medium sized object scan with a maximum error of more than 0.7 is considered as poor quality scan [21].

2.4 Post-processing methods

1
2
3 160 Two post-processing methods were assessed and compared in terms of validity (trueness).
4
5 161 First, the “Autopilot” feature of the software which only allows minimal adjustment of
6
7 162 preferences (S 3). This is the easiest and least time-consuming way to obtain 3D reconstruction
8
9 163 of scans using the software provided by Artec (Studio 12 Professional). Second, the “Manual”
10
11 164 post-processing method which allows modifications of the raw scan data using various
12
13 165 different tools. S 3 gives an overview of the preferences used for autopilot and manually post-
14
15 166 processed scans in accordance with the Artec Studio 12 user guide [17]. A detailed description
16
17 167 of the processing tools can be found as supplementary information S 2.
18

169 Validity

170 Validity (trueness) of the 2 aforementioned post-processing methods was assessed in terms of
171
172 accuracy against actual (real-time) hand measurements. Prior to scanning, black circular self-
173
174 adhesive dots with a diameter of 10 mm were placed onto the dorsal aspect of the human hand.
175
176 The following dots were used as landmarks during the measurement process (Supplementary
177
178 information S 4):

- 175 • Wrist (2 dots)
- 176 • Dorsum of the hand (2 dots)
- 177 • Metacarpophalangeal joint (MCPJ) of index finger (1 dot)
- 178 • Proximal interphalangeal joint (PIPJ) of index finger (1 dot)
- 179 • Distal interphalangeal joint (DIPJ) of index finger (1 dot)

180 The shortest distance between two landmarks was measured using Artec Studio 12 Professional
181
182 (Supplementary information S 4).

183 The hand of one volunteer was scanned three times in each position. Each scan was duplicated
184
185 and processed once using the manual tools and once using the Autopilot tool. Both processed
186
187 scans then underwent measurements in five different hand areas as shown as supplementary
188
189 information S 4. A total of five measurements (one in each hand area) was defined as one
190
191 measurement cycle. Each measurement cycle was performed three times in both manually and
192
193 Autopilot processed scans. (6 hand positions x 3 scans x 2 post-processing methods x 5
194
195 measurements per cycle (Wrist, Dorsum, MCPJ→PIPJ, PIPJ→DIPJ, Fingertip) x 3
196
197 measurement cycles) shown as supplementary information S 5.

198 Scans with a maximum error of over 0.7 A.U. can be seen as poor-quality scans and were
199
200 therefore excluded from the measurement process [21]. The number of polygons was reduced

193 to a maximum of 300,000 (software recommendation) for all scans prior to geodesic
194 measurement.

195 Autopilot and manually post-processed scan measurements were then compared to actual hand
196 dimensions. Actual measurements were performed using photographs of the hand and the
197 software “ImageJ”, except for the fingertip since its measurement path could not be captured
198 in one image (Supplementary information S 4C). A measurement tape was used to directly
199 measure the path between two predefined fingertip landmarks (most proximal point of the
200 fingernail → fingertip → DIPJ flexor crease). Each real-time measurement was performed
201 three times in total (Supplementary information 4C).

202

203 **2.5 Statistical analysis**

204 **2.5.1 Data acquisition methods**

205 Mean and standard deviation of the maximum errors was calculated for both data acquisition
206 methods. An independent t-test ($p < 0.05$, 95% Confidence Interval (CI)) was used to compare
207 the average maximum errors of both data acquisition methods.

208 **2.5.2 Hand scanning positions**

209 Mean of “scanning comfort” and “ease of scanning” evaluation was calculated for each hand
210 position. Spectrum charts were used to illustrate those results. Mean and standard deviation of
211 the maximum error was additionally calculated for each hand scanning position using a two-
212 way analysis of variance (ANOVA).

213 **2.5.3 Post-processing methods**

214 Mean and standard deviation of the hand area measurements were calculated for both
215 intervention groups (Autopilot and Manual) and the control group (Real-time). A two-way
216 analysis of variance (ANOVA) with 95% confidence intervals (CI) was performed to compare
217 the reference with both autopilot and manually post-processed scans. Additionally, the mean
218 percentage error from the criterion measurements was calculated for each hand area for both
219 groups (Autopilot and Manual) and displayed as a graph for each hand position. Hand scanning
220 positions with an average maximum error of over 0.7 are considered poor-quality scans and
221 were therefore discarded and not assessed in the “post-processing” evaluation step.

222 **3. Results**

223 **3.1 Data acquisition method (1-step versus 2-step scanning)**

224 The average maximum error of the 1-step scanning method with a value of 0.5 A.U. (± 0.26
225 SD) was lower than the average maximum error of the 2-step scanning method with a value of

1
2
3 226 1.03 A.U. (± 0.78 SD) (Table 1). An unpaired t-test ($p < 0.05$, CI 95%) was used to compare
4
5 227 the average maximum errors of the two data acquisition methods. However, the difference
6
7 228 between those errors was not statistically significant ($p > 0.35$). The 2-step scans consist of 2
8
9 229 individual scans (first step and second step) resulting in 2 maximum errors per 2-step scan. The
10
11 230 average maximum error of the second steps was higher than the average maximum error of the
12
13 231 first steps within the 2-step scanning method. However, no significant difference was detected
14
15 232 between the first and second steps within the 2-step scanning method using the Mann Whitney
16
17 233 U test.

17 234 The 1-step scanning method was chosen for the rest of the experiments due to its reduced
18
19 235 maximum errors in comparison to the two-step scanning method.

20 236

21 237 **Table 1.** Maximum error of 1-step and 2-step scans as well as the mean and standard deviation (SD) of both scanning techniques (1- and 2-step scanning).

Maximum error	1-step scan (in A.U.)	2-step scan (in A.U.)
1. scan	0.3	0.4
2. scan	0.8	0.8
3. scan	0.4	1.9
Mean	0.5 (± 0.26 SD)	1.03 (± 0.78 SD)

Legend: A.U. = arbitrary unit; SD = standard deviation

23 238

24 239 3.2 Hand scanning positions

25 240 3.2.1 Scanning comfort and ease of scanning

26
27
28
29
30
31
32
33
34 241 P1 and P3 had similar average scanning comfort scores of 2.6 and 2.4, whereas P2 was
35
36 242 considered more uncomfortable for the volunteers with an average score of 1.6. Since P4 and
37
38 243 P5 are the same hand position they had the same scanning comfort score of 4.2. Position 6 was
39
40 244 overall the most comfortable scanning position for the volunteers with an average score of 5.
41
42 245 (Figure 4 “Scanning comfort”).

43
44
45
46
47
48 246 Two users validated the difficulty of performing a hand scan in the six hand scanning position.
49
50 247 P1 seemed to be the most challenging hand scanning position with an average score of 1.5. P2
51
52 248 scored highest together with P6 with an average of 4.5 points. P4 had an average score of 3
53
54 249 points, whereas P5 with an additional string as scanning guide resulted in an average score of
55
56 250 4 points (Figure 4 “Ease of scanning”).

57 251

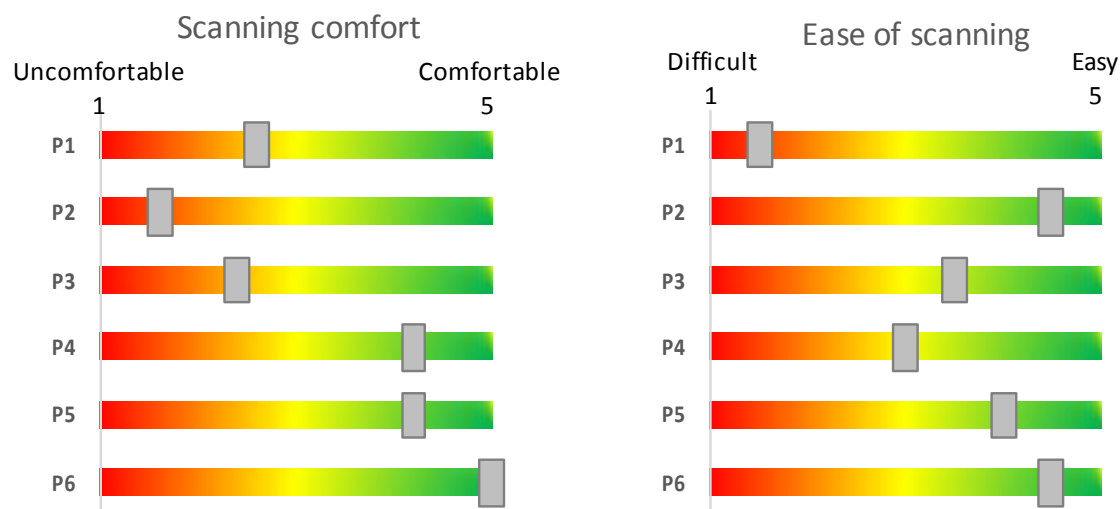


Figure 4. Spectrum chart displaying the results of “scanning comfort” and “ease of scanning” assessment (1: worst / 5: best).

3.2.2 Maximum error

P1 and P4 both had an average maximum error of 0.366 A.U. (± 0.153 SD). P3 and P6 both had an average maximum error of 0.433 A.U. (± 0.058 SD). P5 with a value of 0.33 A.U. (± 0.057 SD) had the lowest maximum error, whereas P2 had the highest value with an average maximum error of 2.23 A.U. (± 1.5 SD). A two-way analysis of variance (ANOVA) showed that the average maximum error of P2 was significantly higher than the average maximum errors of the other five hand positions (Figure 5).

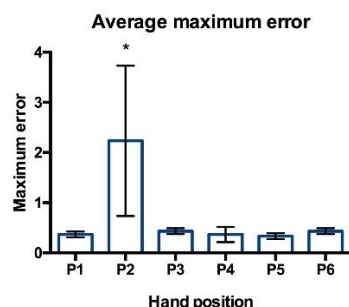


Figure 5. Average maximum error of each hand position. * indicates significant difference.

3.3 Post-processing methods

P2 scans with an average maximum error of 2.23 A.U. exceeded the predefined cut-off of 0.7 A.U. and were therefore excluded from the post-processing evaluation. Furthermore, P2 did not allow any measurements due to its poor scan quality. P6 did not allow any measurements of the ventral fingertip due to its flat surface coverage as shown in Figure 3 (P6).

Validity

The distance between the two landmarks in the wrist and dorsum hand area was significantly decreased in both “Autopilot” and “Manual” post-processed scans for all hand positions

1
2
3 272 compared to real-time measurements. However, the distance between the MCP and PIP joint
4
5 273 was only significantly lower in P1 for both post-processing methods compared to real-time
6
7 274 measurements. The distance between the PIP and DIP joint was not significantly different in
8
9 275 “Autopilot” and “Manual” post-processed scans compared to real-time measurements in any
10
11 276 hand position. Real-time fingertip measurements were similar to “manual” post processing, but
12
13 277 were significantly lower than “Autopilot” post-processed fingertip measurements. (Figure 6 A-
14
15 278 E). The mean distance including all hand positions showed significantly lower values in the
16
17 279 wrist and dorsum area for both post-processing methods, whereas for the fingertip only
18
19 280 “Autopilot” post-processed scans had significantly higher values compared to the reference.
20
21 281 (Figure 6 F)

22
23 282 The calculated percentage errors from real-time measurements showed a tendency towards
24
25 283 higher percentage errors in the more proximal areas (wrist and dorsum) compared to the more
26
27 284 distal areas (MCP-PIP and PIP-DIP) for both post-processing methods amongst all hand
28
29 285 positions, except for the fingertip. The fingertip percentage error from real-time measurements
30
31 286 in Autopilot post-processed scans ranged from -25.11% to -7.43% (mean: -13.85%), whereas
32
33 287 the error from the reference for manually post-processed scans ranged from 0.42% to 5.91%
34
35 288 (mean: 2.8%). The mean percentage error (including P1, P3-P6) of the fingertip showed a
36
37 289 significant difference between the two post-processing methods using an unpaired t-test.
38
39 290 However, average percentage errors of all the other hand areas did not significantly differ
40
41 291 between the two post-processing methods. (Figure 7)

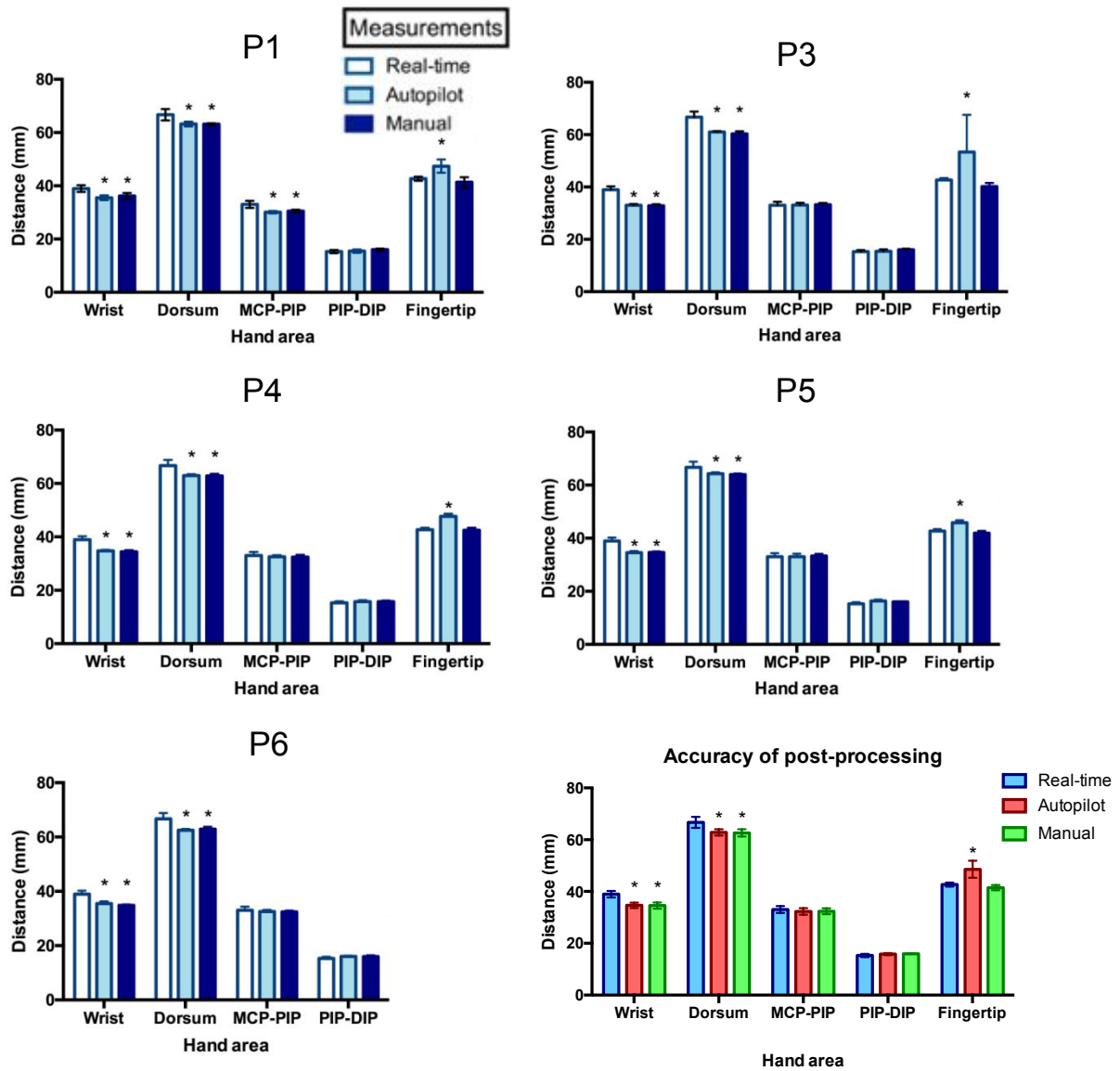


Figure 6. Bar charts assessing the accuracy of anthropometric measurements in different hand areas for both post-processing methods compared to real-time measurement in P1, P3 – P6. Accuracy of both post-processing methods combines P1, P3 – P6. P2 was excluded since it exceeded the predefined maximum error cut-off of 0.7. * indicates significant difference of the respective post-processing method compared to real-time measurement in the same hand area.

292
293
294
295

296

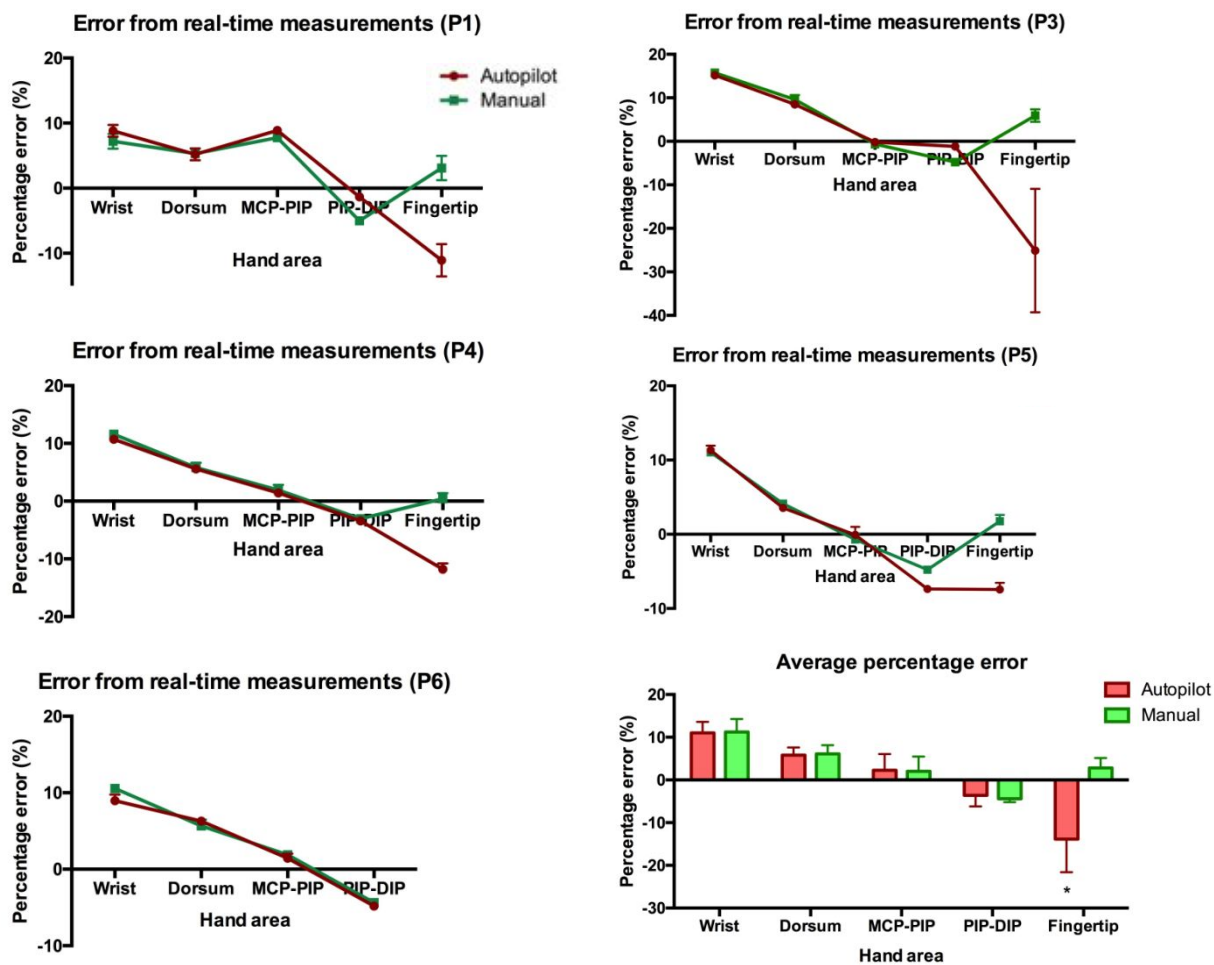


Figure 7. Percentage error from real-time measurements of hand position 1, 3-6 and the average of those 5 hand positions for each hand area. P2 was excluded since it exceeded the predefined cut-off of 0.7 maximum error. * indicates significant difference between the two post-processing methods (Autopilot and Manual). P2 was excluded since it exceeded the predefined maximum error cut-off of 0.7.

297

298

299

300

301

302

303 4. Discussion

304 With the increasing demand of bespoke devices, the use of 3D imaging techniques has gained
305 high interest in various medical fields [1, 19, 22]. Those techniques not only permit to obtain
306 reliable body part models, but also allow to drastically reduce the number of manufactured
307 prototypes. A study group by Aydin et al. showed the potential of using a 3D scanner for the
308 purpose of computer aided custom fitting of a medical device. A 3D model of the foot was
309 obtained using structured light scanning technology. Finite element analysis enabled the
310 simulation of applied forces in order to assess its mechanical properties. This allows validation
311 of quality, performance and safety of a medical device before the manufacture which ultimately
312 saves time and production costs [23]. However, 3D surface scanners for medical applications
313 still give rise to several uncertainties regarding the accuracy, validity and the translation of the
314 scanning process into a clinical scenario. It is essential to obtain a good quality scan which can
315 be implemented into the manufacturing process of 3D printed patient specific devices and to
316 assess its feasibility in a clinical setting. A study group by Chan et al. already assessed such a
317 hand-held structured light scanning technology for 3D knee joint models showing its potential
318 feasibility in an operative setting [24]. The human hand with its complex mechanical and
319 anatomical features potentially causing scanning errors, is considered a challenging object to
320 scan and has so far not been assessed and validated by previous authors.

322 Data acquisition method (1-step versus 2-step scanning)

323 Although, the average maximum error of the 1-step and 2-step scanning technique did not
324 differ significantly, results still showed a tendency towards a reduced scan quality of the 2-step
325 scans with higher maximum errors. Especially the second step within the 2-step scanning
326 technique seems to negatively affect the scan quality with higher maximum errors than the first
327 step in each of the 2-step scans. Furthermore, the 2-step scanning technique can be seen as a
328 more time-consuming and demanding procedure due to the fact that the second step of the 2-
329 step scan requires about 30% information overlap of the first step. In addition, as small hand
330 movements are always present in an individual, it is challenging to re-detect the last 30% of
331 the first scan which gives rise to potential errors.

332 Not only the scanning procedure but also the post-processing of the 2-step scan requires higher
333 skills and more experience than the 1-step scanning technique. The 2 scans of the 2-step
334 scanning technique further need to be manually aligned using a scanning software. This is a
335 challenging task even for more experienced users and can easily cause artefacts. Time and

336 scanning skills are two important factors which shall not be taken for granted in a clinical
337 setting. Therefore, the 1-step scanning technique seems to be more suitable for clinical usage
338 than the 2-step scanning technique.

339 **Hand positions**

340 Even though statistically the population most likely affected from hand injuries ranges from 20
341 to 29 years [25], it is important to consider that such injuries can occur at any age. As a result,
342 it was necessary to find a suitable hand position for the scanning procedure that would take
343 several patient limitations (such as holding the arm in difficult positions for about one minute,
344 or hand movements) as well as scanning errors into account. The evaluation of the best hand
345 scanning position was solely performed with the 1-step scanning technique due to its overall
346 superiority compared to the 2-step scanning technique. P4, P5 and P6 showed to be the most
347 comfortable hand positions from a volunteer's perspective. The effort to keep the hand in a
348 stable position is reduced in those three positions by using supportive devices such as a table
349 or a bed. This seems to make the scanning process more tolerable. Although, the age of the
350 volunteers included in this evaluation (24 to 29 years) matches the most commonly affected
351 age group, adequate positioning of the hand might be even more important for patients at a
352 higher age with limited mobility. Although no elderly volunteer was interviewed yet, P4, P5
353 and P6 are still believed to be the most comfortable positions.

354 The most pleasant hand scanning positions from the users' perspective showed to be P2, P6
355 and P5. Those three positions require minimal physical user effort to capture the whole hand
356 surface. However, P2 had the worst overall scan quality outcome with a maximum error above
357 the cut-off value of 0.7 A.U. This did not allow any reliable measurements of P2 and led to its
358 withdrawal from any further evaluation.

359 Overall, P6 showed encouraging results. However, its major limitation is its coverage of either
360 the dorsal or the ventral aspect of the hand by the underlying surface. Since the development
361 of medical hand devices usually requires information of both aspects, P6 is not considered a
362 feasible hand scanning position.

363 P5 provides an ideal balance between the overall scan quality, duration of scanning, scanning
364 comfort and ease of scanning amongst all hand positions. The application of a string guide
365 seems to make the scanning process easier and less time-consuming for the user. The string
366 allows to maintain consistent distance of the scanner to the scanned object resulting in a higher
367 scan quality. Taking all those results into account, P5 is considered as the ideal hand position
368 to perform a hand scan in a clinical setting.

369 **Post-processing methods**

370 Various different studies have assessed the measurement accuracy of structured-light surface
371 scanned body parts such as breasts, face or limbs comparing it with other scanning techniques
372 or direct measurements [18, 19, 26-28]. However, to the best of our knowledge, this is the first
373 study so far assessing the validity of 3D hand surface scans. In terms of valid measurements
374 two predefined post-processing methods were assessed and compared with real-time
375 measurements as reference in this study.

376 Both post-processing methods showed to decrease the hand surface in the more proximal hand
377 areas up to more than 10%. Smoothing tools, which even out noisy areas in both post-
378 processing methods, might have caused the reduction of the surface area in the more proximal
379 hand areas. Reference measurements performed with “ImageJ” could have overstated the
380 distance in the proximal area contributing to the significant effect. Nevertheless, hand surface
381 reduction needs to be taken into account and quantified when using 3D hand scan as template
382 for the design and development of medical devices. In contrast, Modabber et al. and Lauer et
383 al. assessed the validity of facial measurements using three-dimensional surface scans and
384 comparing it to direct measurements of certain areas in the face using a measurement tape.
385 Their results showed highly accurate measurements without any significant deviation to the
386 reference. The fact that the face is less subjected to movements, might have required less post-
387 processing of the scan causing less surface reduction [26, 29].

388 The increased distance of the fingertip obtained from the Autopilot post-processed scans
389 compared to manually post-processed scans can be explained by artefacts. Autopilot post-
390 processed scans were also more likely to cause artefacts in other complex hand surface areas
391 such as the interdigital web space. Such artefacts can affect measurements and require manual
392 removal with an imaging software. In general, the main benefit of the Autopilot feature is that
393 it hardly requires any software skills and is less-time consuming than the manual post-
394 processing method. However, the user is very limited with the Autopilot feature in terms of
395 processing modifications.

396 On the other hand, with manually post-processed scans, the user is aware of all operations and
397 their magnitudes performed on the scan and always has the option to individually tailor them
398 if the outcome is not ideal. The user can thus modify the scan as much needed to obtain an
399 optimal result. As a consequence, the presence of major errors and artefacts is limited and
400 dependent on the user.

401

1
2
3 402 The overall aim of this study was to perform a high quality three-dimensional hand surface
4 scan in a highly comfortable position for the scanned person and at the same time making the
5 403 scanning process as easy as possible for the user. Obtaining a quality scan in the most efficient
6 404 way is important as this ultimately can be used as a template for the design and development
7 405 of a 3D printed patient specific medical device. Taking all those scanning evaluation results
8 406 into consideration, a manually post-processed 1-step scan in P5 “Minimal force plus guide”
9 407 can meet those requirements to the highest extent.
10 408
11 409

17 410 **5. Conclusion**

19 411 This study shows the potential of obtaining a 3D hand scan subsequently used for the design
20 412 of a bespoke 3D printed medical device. To our knowledge, no study so far has addressed
21 413 uncertainties and challenges occurring before and during the scan of a complex structure like
22 414 the hand. Results lead to the recommendation of performing manually post-processed 1-step
23 415 scans in a hand position of minimal patient effort with the use of a scanning guide.
24 416

29 417 **6. Future Perspective**

31 418 This study shows potential for acquiring high resolution 3D hand surface scans within a clinical
32 419 setting which can then be used for the development of customised medical devices. Previously
33 420 published studies showed that such a technology can also be applied to other parts of the human
34 421 body. Various different software tools such as surface measurement and finite element analysis
35 422 of the 3D model can simplify the prototyping process of bespoke devices which ultimately
36 423 saves time and money.
37 424

43 425 **7. Summary Points**

- 45 426 • This study aims to obtain high quality 3D hand surface scans by developing a feasible
46 427 and reliable scanning protocol using laser free structured light surface scanning
47 428 technology
- 49 429 • Different parameters such as data acquisition methods, hand positions and post-
50 430 processing methods were compared in order to assess the hand scan with the highest
51 431 quality.
- 52 432 • Results show that a manually post-processed 1-step scan in the position “Minimal force
53 433 plus guide” can meet those requirements to the highest extent

1
2
3
4
5
6
7
8
9
10
11
12
13
14
15
16
17
18
19
20
21
22
23
24
25
26
27
28
29
30
31
32
33
34
35
36
37
38
39
40
41
42
43
44
45
46
47
48
49
50
51
52
53
54
55
56
57
58
59
60

- 434 • This optimised scanning protocol enables the acquisition of high quality surface scans
435 which can help to design and develop patient specific devices, reduce number of
436 prototyping and ultimately save time and production costs.

For Review Only

438 **Figure legends**

439 **Figure 1.** Flow chart of the proposed method.

440 **Figure 2.** Data acquisition methods. **A.** One-step method: one continuous scan orbiting the handheld scanner 360°
441 around the hand; **B.** Two-step method: the scanning process is divided into two 180° orbits. One scan captures the
442 dorsal aspect of the hand (1) and the other scan the palmar aspect of the hand (2). The volunteer was advised to stand
443 upright, perform a combined arm elevation to 90° and hold this position during the entire scanning process with the
444 least possible hand movement.

445 **Figure 3.** Figurative representation of the Hand scanning positions. **P1.** 90° arm elevation; **P2.** 90° arm elevation with
446 full hand rotation; **P3.** 180° arm elevation; **P4.** Minimal force; **P5.** Minimal force plus guide; **P6.** Hand on surface.
447 **Blue** indicates moving scanner; **red** indicates hand rotation.

448 **Figure 4.** Spectrum chart displaying the results of “scanning comfort” and “ease of scanning” assessment (1: worst /
449 5: best).

450 **Figure 5.** Average maximum error of each hand position. * indicates significant difference.

451 **Figure 6.** Bar charts assessing the accuracy of anthropometric measurements in different hand areas for both post-
452 processing methods compared to real-time measurement in P1, P3 – P6. Accuracy of both post-processing methods
453 combines P1, P3 – P6. P2 was excluded since it exceeded the predefined maximum error cut-off of 0.7. * indicates
454 significant difference of the respective post-processing method compared to real-time measurement in the same hand
455 area.

456 **Figure 7.** Percentage error from real-time measurements of hand position 1, 3-6 and the average of those 5 hand
457 positions for each hand area. P2 was excluded since it exceeded the predefined cut-off of 0.7 maximum error. *
458 indicates significant difference between the two post-processing methods (Autopilot and Manual). P2 was excluded
459 since it exceeded the predefined maximum error cut-off of 0.7.

460

1
2
3
4
5
6
7
8
9
10
11
12
13
14
15
16
17
18
19
20
21
22
23
24
25
26
27
28
29
30
31
32
33
34
35
36
37
38
39
40
41
42
43
44
45
46
47
48
49
50
51
52
53
54
55
56
57
58
59
60

461 **Table legends**

462 **Table 1.** Maximum error of 1-step and 2-step scans as well as the mean and standard deviation (SD) of both scanning
463 techniques (1- and 2-step scanning).

464
465
466

For Review Only

467 **References**

- 468 1. Treleaven P, Wells J. 3D Body Scanning and Healthcare Applications. *Computer* 40(7),
 469 28-34 (2007).
- 470 2. Geng J. Structured-light 3D surface imaging: a tutorial. *Advances in Optics and*
 471 *Photonics* 3(2), 128-160 (2011).
- 472 3. R.M. JP, Peng L, Katherine BW, M. WG. Format for human body modelling from 3-D
 473 body scanning. *International Journal of Clothing Science and Technology* 7(1), 7-16
 474 (1995).
- 475 4. Demers MH, Hurley JD, Wulpern RC, Grindon JR. *Three dimensional surface capture*
 476 *for body measurement using projected sinusoidal patterns*. 3023, (1997).
- 477 5. Tzou CH, Artner NM, Pona I *et al*. Comparison of three-dimensional surface-imaging
 478 systems. *J Plast Reconstr Aesthet Surg* 67(4), 489-497 (2014).
- 479 6. Tokkari N, Verdaasdonk RM, Liberton N *et al*. Comparison and use of 3D scanners to
 480 improve the quantification of medical images (surface structures and volumes) during
 481 follow up of clinical (surgical) procedures. In: *Advanced Biomedical and Clinical*
 482 *Diagnostic and Surgical Guidance Systems Xv*, Mahadevanjansen A, Vodinh
 483 T, Grundfest WS (2017).
- 484 7. Treleaven P. Sizing us up. *IEEE Spectrum* 41(4), 28-31 (2004).
- 485 8. Schmitz A, Gabel H, Weiss HR, Schmitt O. [Anthropometric 3D-body scanning in
 486 idiopathic scoliosis]. *Z Orthop Ihre Grenzgeb* 140(6), 632-636 (2002).
- 487 9. Yu CY, Lo YH, Chiou WK. The 3D scanner for measuring body surface area: a
 488 simplified calculation in the Chinese adult. *Appl Ergon* 34(3), 273-278 (2003).
- 489 10. Farrar E, Pujji O, Jeffery S. Three-dimensional wound mapping software compared to
 490 expert opinion in determining wound area. *Burns* 43(8), 1736-1741 (2017).
- 491 11. Lei C, Phan A, Allison G. Design and fabrication of a three dimensional printable non-
 492 assembly articulated hand exoskeleton for rehabilitation. *Conf Proc IEEE Eng Med*
 493 *Biol Soc* 2015 4627-4630 (2015).
- 494 12. ExoHand. *Human-machine cooperation* 4 (2012).
- 495 13. Bataller A, Cabrera JA, Clavijo M, Castillo JJ. Evolutionary synthesis of mechanisms
 496 applied to the design of an exoskeleton for finger rehabilitation. *Mechanism and*
 497 *Machine Theory* 105 31-43 (2016).
- 498 14. Ertas IH, Hocaoglu E, Patoglu V. AssistOn-Finger: An under-actuated finger
 499 exoskeleton for robot-assisted tendon therapy. *Robotica* 32(8), 1363-1382 (2014).
- 500 15. Patoglu V, Ertek G, Öz O, Zoroğlu D, Kremer G. Design requirements for a tendon
 501 rehabilitation robot: results from a survey of engineers and health professionals. *ASME*
 502 *2010 International Design Engineering Technical Conferences & Computers and*
 503 *Information in Engineering Conference (IDETC/CIE 2010), Monreal, Quebec, Canada*
 504 (2010).
- 505 16. Artec Eva specifications. (2018).
- 506 17. Artec3d. User Guide Artec Studio 12. (2017).
- 507 18. Seminati E, Canepa Talamas D, Young M, Twiste M, Dhokia V, Bilzon JLJ. Validity
 508 and reliability of a novel 3D scanner for assessment of the shape and volume of
 509 amputees' residual limb models. *PLoS ONE* 12(9), e0184498 (2017).
- 510 19. Coltman CE, Mcghee DE, Steele JR. Three-dimensional scanning in women with large,
 511 ptotic breasts: implications for bra cup sizing and design. *Ergonomics* 60(3), 439-445
 512 (2017).
- 513 20. Yamamoto S, Miyachi H, Fujii H, Ochiai S, Watanabe S, Shimozato K. Intuitive Facial
 514 Imaging Method for Evaluation of Postoperative Swelling: A Combination of 3-

- 1
2
3 515 Dimensional Computed Tomography and Laser Surface Scanning in Orthognathic
4 516 Surgery. *J Oral Maxillofac Surg* 74(12), 2506 e2501-2506 e2510 (2016).
5 517 21. Artecscan. Max error/Quality value. (2017).
6 518 22. Baronio G, Volonghi P, Signoroni A. Concept and Design of a 3D Printed Support to
7 519 Assist Hand Scanning for the Realization of Customized Orthosis. *Appl Bionics*
8 520 *Biomech* 2017 8171520 (2017).
9 521 23. Aydin L, Kucuk S. A method for more accurate FEA results on a medical device
10 522 developed by 3D technologies. *Polymers for Advanced Technologies* 29(8), 2281-2286
11 523 (2018).
12 524 24. Chan B, Auyeung J, Rudan JF, Ellis RE, Kunz M. Intraoperative application of hand-
13 525 held structured light scanning: a feasibility study. *Int J Comput Assist Radiol Surg*
14 526 11(6), 1101-1108 (2016).
15 527 25. De Jong JP, Nguyen JT, Sonnema AJ, Nguyen EC, Amadio PC, Moran SL. The
16 528 incidence of acute traumatic tendon injuries in the hand and wrist: a 10-year population-
17 529 based study. *Clin Orthop Surg* 6(2), 196-202 (2014).
18 530 26. Modabber A, Peters F, Kniha K *et al.* Evaluation of the accuracy of a mobile and a
19 531 stationary system for three-dimensional facial scanning. *J Craniomaxillofac Surg*
20 532 44(10), 1719-1724 (2016).
21 533 27. Verhulst A, Hol M, Vreeken R, Becking A, Ulrich D, Maal T. Three-Dimensional
22 534 Imaging of the Face: A Comparison Between Three Different Imaging Modalities.
23 535 *Aesthet Surg J* 38(6), 579-585 (2018).
24 536 28. Luhmann T. *3D imaging: how to achieve highest accuracy*. SPIE, 8085, EOM (2011).
25 537 29. Lauer EA, Corner BD, Li P, Beecher RM, Deutsch C. Repeated-measure validation of
26 538 craniofacial metrics from three-dimensional surface scans: application to medical
27 539 genetics. Presented at: *Electronic Imaging*. 2002.
28 540
29
30
31
32
33
34
35
36
37
38
39
40
41
42
43
44
45
46
47
48
49
50
51
52
53
54
55
56
57
58
59
60

Supplementary information

S 1

Description of each hand scanning position. In each position, except P2, the volunteer was instructed to move the hand as little as possible since movements are known to affect the overall scanning result. In P2 the volunteer was instructed to rotate the arm and hand 360° while the scanner remains in a fixed position.

Label	Position	Description
P1	90° arm elevation	upright standing position - combined arm elevation to 90° - arm kept stable - scanner orbits around the hand
P2	90° arm elevation with full hand rotation ("90° mvt")	upright standing position - combined arm elevation to 90° - combined full 360° arm and hand rotation - scanner remains in a fixed position
P3	180° arm elevation	upright standing position - combined arm elevation to 180° - arm kept stable - scanner orbits around the hand
P4	Minimal force	prone position on an elevated surface - arm points downwards with minimal effort - scanner orbits around the hand below the bed
P5	Minimal force plus guide	prone position on an elevated surface - arm points downwards with minimal effort - scanner is attached to a string acting as guidance - scanner orbits around the hand below the bed
P6	Hand on surface	palmar aspect of hand is placed on flat surface - hand kept stable - scanner moves from ulnar to radial and from wrist to finger tips

S 2

“**Global registration**” converts all frames into one single coordinate system. “registration_algorithm” was set to “Geometry mode” for objects with rich geometry. “minimal distance” is the minimum distance between adjacent feature points in millimetres and was set to 0.3 mm. The number of iterations of the global optimization algorithm was set to 2000.[17] Outliers which are small surfaces not connected to the main surfaces can arise during the scanning process. This affects the model and can produce unwanted shapes or fragments. “**Outlier removal**” is a tool to remove those outliers. A standard-deviation multiplier value of 2 was chosen since this is the recommended value for noisier surfaces.[17] There are two ways to remove outliers: either before fusion or after fusion. In this study, outliers were removed before fusion since this is recommended by Artec 3D®.[17]

1
2
3
4
5
6
7
8
9
10
11
12
13
14
15
16
17
18
19
20
21
22
23
24
25
26
27
28
29
30
31
32
33
34
35
36
37
38
39
40
41
42
43
44
45
46
47
48
49
50
51
52
53
54
55
56
57
58
59
60

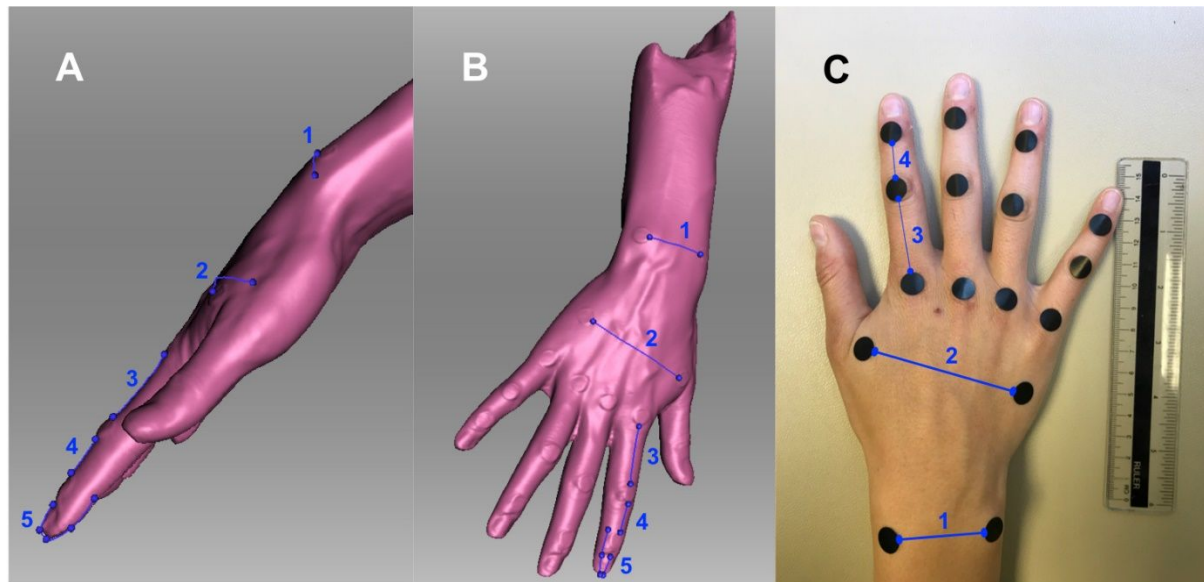
“**Fusion**” is a feature which melts and solidifies the captured and processed frames resulting in a polygonal 3D model. The software offers three different algorithms: fast, smooth and sharp fusion. Smooth fusion is the algorithm of choice for human bodies since it is able to compensate for slight movements by the person.[17] The resolution was set to 0.5 mm and the parameter “watertight”, which automatically fills all the holes in the mesh was used for the hand scans in this study. Prior to both processing methods (“Autopilot” and “Manual”) an “**Eraser**” tool was used to eliminate unwanted elements or objects.

S 3 Autopilot and Manual processing preferences.

Autopilot		Manual	
Scan quality	Good	Global Registration	
Object size	Medium	registration algorithm	Geometry
Hole-filling method	Watertight	minimal distance	0.3
Model resolution	0.5	iterations	2000
Polygon count	Auto	Outlier removal	
		std_dev_mul_threshold	2
		resolution	1
		Smooth fusion	
		resolution	0.5
		fill_holes	Watertight
		remove targets	Off

S 4

Illustration of anthropometric measurements using a 3D hand scan (**A.** side view; **B.** front view) and **C.** a real-time image; Measurements were performed at the following five hand areas: **1.** Wrist, **2.** Dorsum of the hand, **3.** MCPJ → PIPJ, **4.** PIPJ → DIPJ, **5.** Fingertip (most proximal point of the fingernail → most distal part of the fingertip → DIPJ flexor crease).



S 5

Measurement cycle for each hand position. red circle encloses the 5 hand areas which equals one measurement cycle.

